iScience

CellPress
OPEN ACCESS

Article

HAMSAB diet ameliorates dysfunctional signaling in pancreatic islets in autoimmune diabetes

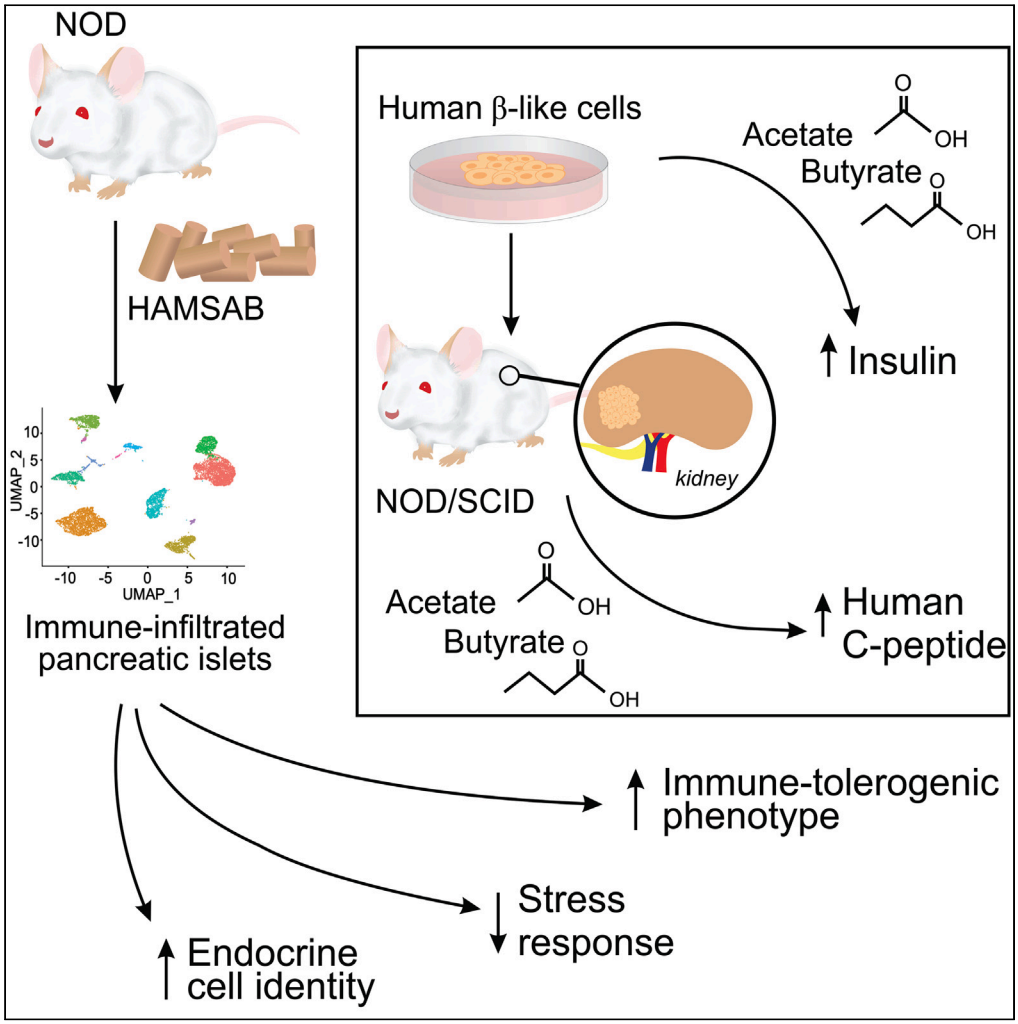

Valerie Vandenbempt, Sema Elif Eski, Manoja K. Brahma, ..., Eliana Mariño, Conny Gysemans, Esteban N. Gurzov

esteban.gurzov@ulb.be

Highlights

HAMSAB induces a tolerogenic phenotype of infiltrated immune cells in NOD mice

HAMSAB reduces the stress response maintaining endocrine cell identity in NOD mice

SCFAs increase insulin levels and function of human beta-like cells

HAMSAB is an attractive strategy for clinical studies in early type 1 diabetes

Vandenbempt et al., iScience 27, 108694
January 19, 2024
https://doi.org/10.1016/j.isci.2023.108694

iScience

CellPress
OPEN ACCESS

Article

HAMSAB diet ameliorates dysfunctional signaling in pancreatic islets in autoimmune diabetes

Valerie Vandenbempt,[1] Sema Elif Eski,[2] Manoja K. Brahma,[1] Ao Li,[1] Javier Negueruela,[1] Ylke Bruggeman,[3] Stéphane Demine,[1] Peng Xiao,[4] Alessandra K. Cardozo,[4] Nicolas Baeyens,[5] Luciano G. Martelotto,[6] Sumeet Pal Singh,[2] Eliana Mariño,[7,8] Conny Gysemans,[3] and Esteban N. Gurzov[1,9,10,*]

SUMMARY

An altered gut microbiota is associated with type 1 diabetes (T1D), affecting the production of short-chain fatty acids (SCFA) and glucose homeostasis. We previously demonstrated that enhancing serum acetate and butyrate using a dietary supplement (HAMSAB) improved glycemia in non-obese diabetic (NOD) mice and patients with established T1D. The effects of SCFA on immune-infiltrated islet cells remain to be clarified. Here, we performed single-cell RNA sequencing on islet cells from NOD mice fed an HAMSAB or control diet. HAMSAB induced a regulatory gene expression profile in pancreas-infiltrated immune cells. Moreover, HAMSAB maintained the expression of β-cell functional genes and decreased cellular stress. HAMSAB-fed mice showed preserved pancreatic endocrine cell identity, evaluated by decreased numbers of poly-hormonal cells. Finally, SCFA increased insulin levels in human β-like cells and improved transplantation outcome in NOD/SCID mice. Our findings support the use of metabolite-based diet as attractive approach to improve glucose control in T1D.

INTRODUCTION

Type 1 diabetes (T1D) is an autoimmune disease caused by T cell mediated destruction of insulin-producing β cells in the pancreatic islets of Langerhans.[1] Short-chain fatty acids (SCFAs), like acetate, propionate and butyrate, are products of bacterial fermentation and have many anti-inflammatory, anti-microbial, and pro-metabolic properties.[2] Several studies using highly sensitive multi-omics technologies have detected significant changes in the gut microbiota, leading to reduced serum SCFAs concentrations associated with clinical disease.[3–6] The pathogenesis of T1D is linked to dysbiosis, characterized by dysregulated production of microbial metabolites.[6,7] We have recently shown in germ-free mice that autoimmune diabetes development was linked to gut microbial defects, including the ability to produce SCFAs.[8]

Diet is one of the main factors that affects microbiota-host interactions resulting in metabolite changes, which can be found in T1D.[9,10] The use of crude dietary fiber does not allow the assessment of specific SCFAs in the mechanism of action of autoimmune diabetes. Thus, we have developed a specialized diet that after bacterial fermentation in the colon releases large amounts of acetate and butyrate.[8] The acetylated and butyrylated, high-amylose, maize-resistant starch (HAMSAB) diet provides advantages over oral administration of SCFAs, which does not model their absorption from the colon through bacterial fermentation of dietary fiber. Importantly, HAMSAB prevented T1D development in the non-obese diabetic (NOD) mouse model.[8] This SCFA-mediated autoimmune diabetes protection occurred via complementary pathways – by expanding regulatory (Treg) T cells (butyrate dependent) and diminishing frequencies of pathogenic B cells, $CD4^+$, and $CD8^+$ T cells (acetate dependent). Remarkably, the human trial with HAMSAB in patients with established T1D replicated some of the same encouraging findings in the preclinical mouse model. Indeed, changes in microbiota composition and function (metagenomics) were correlated with improved glycemic control.[6] Furthermore, an enhanced Treg profile, reduced co-stimulatory CD86 expression in B cells and other antigen-presenting cells

[1]Signal Transduction and Metabolism Laboratory, Université libre de Bruxelles, 1070 Brussels, Belgium
[2]IRIBHM, Université libre de Bruxelles, 1070 Brussels, Belgium
[3]Clinical and Experimental Endocrinology (CEE), Department of Chronic Diseases, Metabolism and Ageing (CHROMETA), Campus Gasthuisberg O&N 1, KU Leuven, 3000 Leuven, Belgium
[4]Inflammatory and Cell Death Signaling in Diabetes group, Signal Transduction and Metabolism Laboratory, Université libre de Bruxelles, 1070 Brussels, Belgium
[5]Laboratoire de Physiologie et de Pharmacologie, Université Libre de Bruxelles, 1000 Brussels, Belgium
[6]Single Cell and Spatial-Omics Laboratory, Adelaide Centre of Epigenetics, University of Adelaide, Adelaide, SA 5005, Australia
[7]Infection and Immunity Program, Biomedicine Discovery Institute, Department of Biochemistry, Monash University, Melbourne, VIC 3800, Australia
[8]ImmunoBiota Therapeutics Pty Ltd, Melbourne, VIC 3187, Australia
[9]WELBIO Department, WEL Research Institute, Avenue Pasteur 6, 1300 Wavre, Belgium
[10]Lead contact
*Correspondence: esteban.gurzov@ulb.be
https://doi.org/10.1016/j.isci.2023.108694

were observed. Collectively, HAMSAB elicited personalized phenotypic immune changes in the blood, indicative of increased immune tolerance.[6] This finding underscored the therapeutic potential of the HAMSAB supplement.

Our preclinical and clinical studies have shown HAMSAB to be a potent modulator of the immune system. SCFAs reduce the destruction of insulin-producing β cells and inhibit or ameliorate disease progression.[11,12] Several studies have also investigated the beneficial effects of SCFAs in pancreatic human and rodent β cells and islets *in vitro*.[13–16] However, the role of acetate and butyrate in endocrine cells is still unclear. No previous studies have assessed *in vivo* gene expression changes induced by SCFAs in immune-infiltrated pancreatic islets.

Here, we assessed the effects of a short administration of HAMSAB diet in our NOD colony.[8] Additionally, using a highly diabetogenic protein-based rodent diet (NIH-31M), we demonstrated that HAMSAB supplementation had significant effects on immune-infiltrated islet cells. HAMSAB reduced stress response gene expression and maintained gene expression of functional islet endocrine cells, contributing to the protective effect of HAMSAB on diabetes development. Our findings highlight immune and endocrine cell pathways that may underline autoimmune diabetes. Furthermore, our results support the potential of a dietary approach based on SCFA to improve glucose control in T1D.

RESULTS

Short-term administration of acetylated and butyrylated starch trends to reduce autoimmune diabetes incidence in non-obese diabetic (NOD) mice

We aimed to perform single-cell RNA sequencing analysis of immune-infiltrated pancreatic islet cells. To perform islet isolation before β-cell destruction and diabetes onset in the control mice, we altered the original 10-week protocol[8] for a shorter 5-week HAMSAB/HAMS feeding regimen. First, we assessed whether HAMSAB supplementation exerted protective effects on autoimmune diabetes development with a natural ingredient diet (NIH-31M). Given that the NIH-31M diet is known to be highly diabetogenic in NOD mice (Taconic Biosciences), 5-week-old female NOD mice were fed for 5 weeks with a blended/mixed HAMSAB or HAMS with NIH-31M, instead of the previously used purified formulation (AIN-93G).[8] As expected, the HAMSAB diet reduced diabetes incidence in 6/13 female NOD mice compared to 11/14 female NOD mice fed with the HAMS control diet (Figure 1A), in line with previous observations.[8] Interestingly, individual blood glucose measurements revealed unusual oscillatory glucose concentrations in HAMSAB-fed mice, suggesting that HAMSAB supplementation may help pancreatic β cells in resisting immune attack (Figure 1B). After 5 weeks of HAMSAB diet administration, female NOD mice had a similar body weight to control diet and HAMS diet mice (Figure 1C). Additionally, no differences were observed in lean/fat mass body composition (Figure 1D).

We found that a greater number of mice fed HAMSAB diet were protected from diabetes, compared to control HAMS diet mice. However, contrary to previous findings, HAMSAB when mixed with NIH-31M diet did not significantly delay global insulitis development after 5 weeks of feeding (Figure 1E). Insulin levels measured at this early time point had a trend to increase in HAMSAB-fed mice, albeit not significantly (Figure 1F). HAMSAB treatment showed similar trends despite the strength of the diabetogenic dietary component.

Next, we aimed to determine whether the protective effects of the HAMSAB diet were attributed to changes in diversity and gene expression in early immune-infiltrated pancreatic islets. We therefore performed single-cell RNA sequencing in isolated islets to assess further changes in transcription and translation in islets that could explain the differences between HAMSAB- and HAMS-fed mice. We mapped the gene expression profiles of 4,750 and 4,117 individual islet cells from HAMSAB- or HAMS-fed mice, respectively, with a similar nCount/nFeature after normalization (Figure S1A). The stage selected for analysis corresponded to a progressive increase in intra-islet leukocyte infiltration. It also represents a time when immune infiltration is prominent in most islets, without dysglycemia.[17,18] We identified the major immune and endocrine cell populations (Figure 1G) by PCA and graph-based clustering, using Shared Nearest Neighbor (SNN). Cell identity was assigned in a supervised manner, based on hallmark gene expression in different cell populations (Figure 1H).[18]

The highest intra-islet infiltrate was represented by T cells, B cells, and classical dendritic cells (cDCs), in line with a previous report.[18] Interestingly, cDCs frequencies were higher in islets from HAMS compared to HAMSAB islet cells (31 vs. 18% respectively, Figure 1I) similar to what was observed in our phase 1 study in patients with established type 1 diabetes.[6] The HAMSAB-fed mice showed a slightly higher percentage of endocrine cells (47.4% vs. 42.6%) in islets. Remarkably, the distribution was different between cell types: 28% and 25% in β cells (*Ins1*, *Ins2*), 14% and 6% in α cells (*Gcg*), 5% and 10% in δ cells (*Sst*) and 0.4% and 1.6% in PP cells (*Ppy*) in HAMSAB and HAMS islets, respectively (Figure 1I). The free fatty acid receptors were differentially expressed in the cell populations (Figure S1B). From the different cell populations, T cells, B cells, and a small percentage of cDCs demonstrated proliferation signature markers for G2/M and S cell cycle phases (Figure 1J). No difference was observed in total cell proliferation signatures between the diets (data not shown).

We compared our dataset with a single-cell RNA sequencing performed on FACS-enriched infiltrated immune cells in the islets of NOD mice at 4, 8, and 15 weeks of age.[18] Immune and endocrine populations (Macrophages, T cells, B cells, cDC, pDC, β cells, α cells and δ cells) were identified according to identity genes (Figures 2A and 2B). As expected, a higher number of immune cells and lower number of endocrine cells were observed due to FACS-enrichment, compared to the HAMS/HAMSAB islet cells (Figure 2C). Four subtypes of T cells were found after integration (Figure 2D). Identity genes identified CD4 T cells (*Cd4*), CD8 T cells (*Cd8a, Klrc1, Gzmk*), Natural killer cells (*Eomes*) and Natural killer T cells (*Cd3e, Trac*) (Figure 2E). The validation of the different subpopulations is relevant for the subsequent comparison between HAMSAB and HAMS islet cells. To assess possible interactions among immune and endocrine cells, cell-to-cell communication analysis was performed based on connecting receptors and ligands databases by CellPhoneDB.[19] Interestingly, a reduced expression of receptor-ligands was observed in immune-endocrine cells associated with diabetes development and immune system modulation in the HAMSAB compared to HAMS control islets (Figure 2F). We observed reduced ligand-receptor expression of adrenomedullin (*Adm*), which binds to receptor activity-modifying proteins 3 (*Ramp3*) and has been linked to β-cell dysfunction.[20,21] Consistent with HAMS islet cells, bone

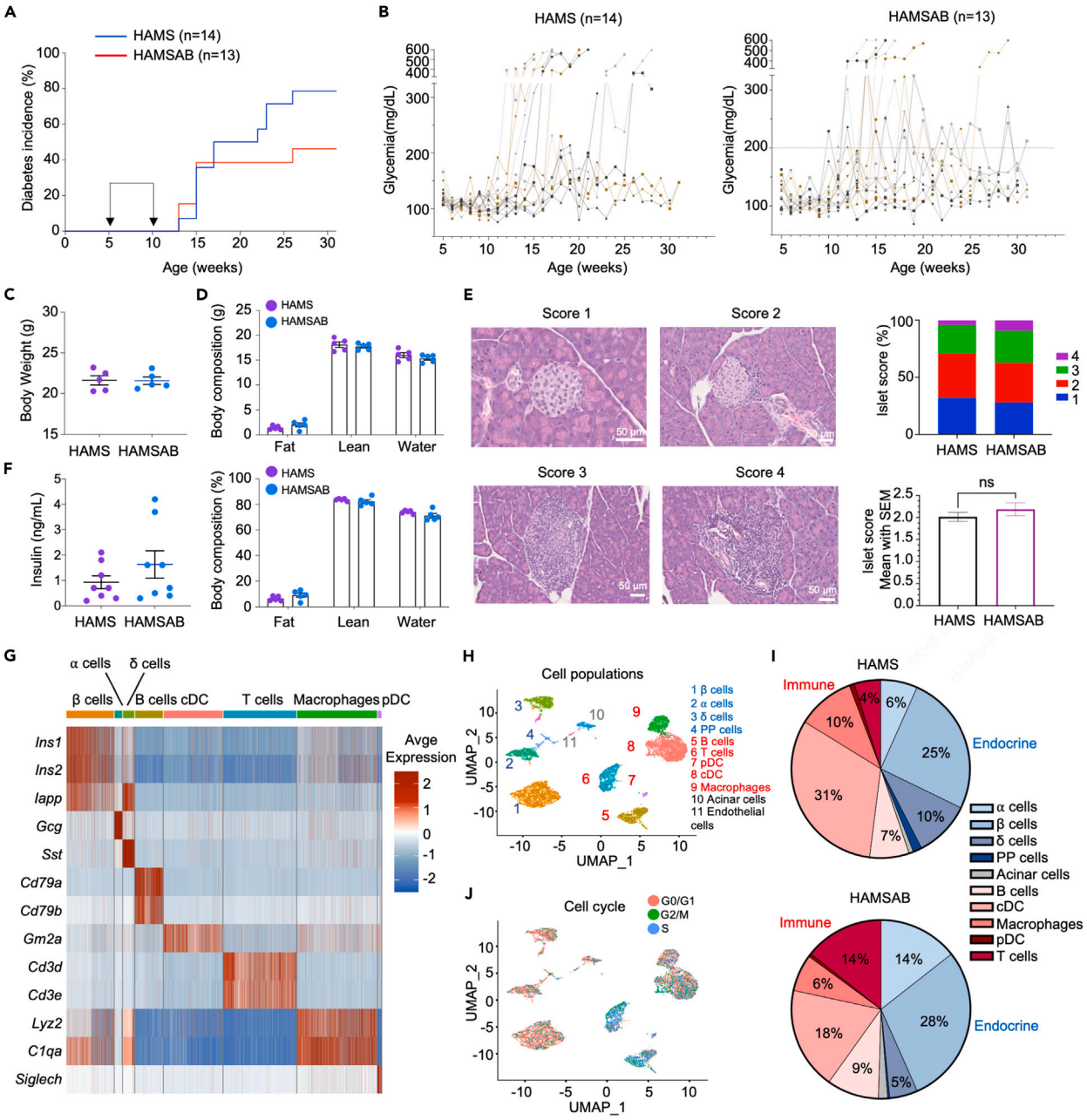

Figure 1. Short-term HAMSAB-feeding trends to reduce diabetes in NOD mice and single-cell RNA sequencing reveals different numbers of immune islet infiltration in HAMSAB and HAMS control islets

(A) Incidence of autoimmune diabetes development in female NOD mice fed HAMS diet (n = 14) or HAMSAB diet (n = 13) for 5 weeks.

(B) Individual glycemia of HAMSAB- and HAMS-fed mice (n = 13–14).

(C) 5-week-old NOD female mice were fed with HAMSAB or HAMS diet for 5 weeks and body weights were determined (n = 5).

(D) Body composition (fat mass, lean mass, and water) was determined 5 weeks after feeding (n = 5).

(E) Microscopy (left) of islets from female NOD mice fed HAMS or HAMSAB diet, and insulitis score (right). Scale bar: 50µm. Data is representative of two independent experiments (40–70 islets were scored per experiment).

(F) Insulin levels were assessed by ELISA (n = 8).

(G) Islets from NOD mice fed the HAMS or HAMSAB diet were harvested and subjected to single-cell RNA sequencing analysis (n = 4). The identity genes were used to annotate the cell populations of immune and endocrine cell populations.

(H) UMAP of the detected populations after doublet removal.

(I) The percentages of the cell populations are shown in a pie chart for HAMS- and HAMSAB-fed mice.

(J) Proliferation markers were used to score all single cells for the G1, G2M or S phase. Data are presented as mean ± standard error of the mean (SEM).

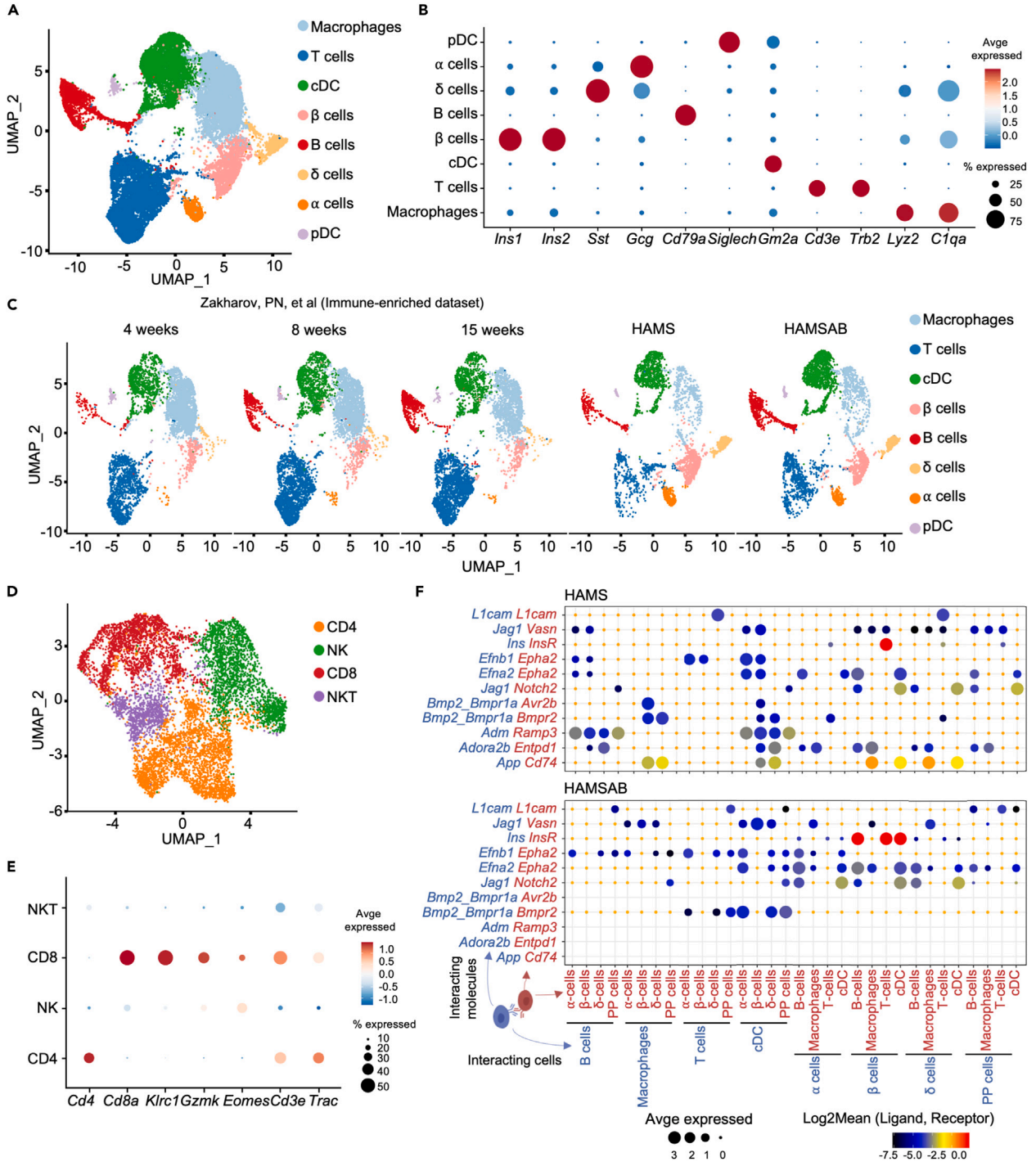

Figure 2. Dataset integration confirms islet cell populations in NOD mice and cell-to-cell communication suggests reduced immune-endocrine cell interaction in HAMSAB compared to HAMS

(A) Integrated UMAP of immune and endocrine cells in NOD mice at different ages.

(B) Dot plot showing cell annotation of the integrated dataset.

(C) Dimension reduction UMAP of the different biological conditions.

(D) T cells exhibit 4 subpopulations.

(E) T cell subtypes are identified with key markers for natural killer T cells (*Cd3e*, *Trac*), $CD8^+$ cells (*Cd8a*, *Klrc1*, *Gzmk*), natural killer cells (*Eomes*) and $CD4^+$ cells (*Cd4*, *Cd3e*, *Trac*).

(F) Cell-to-cell communication calculated by CellPhoneDB in HAMSAB and HAMS islet cells.

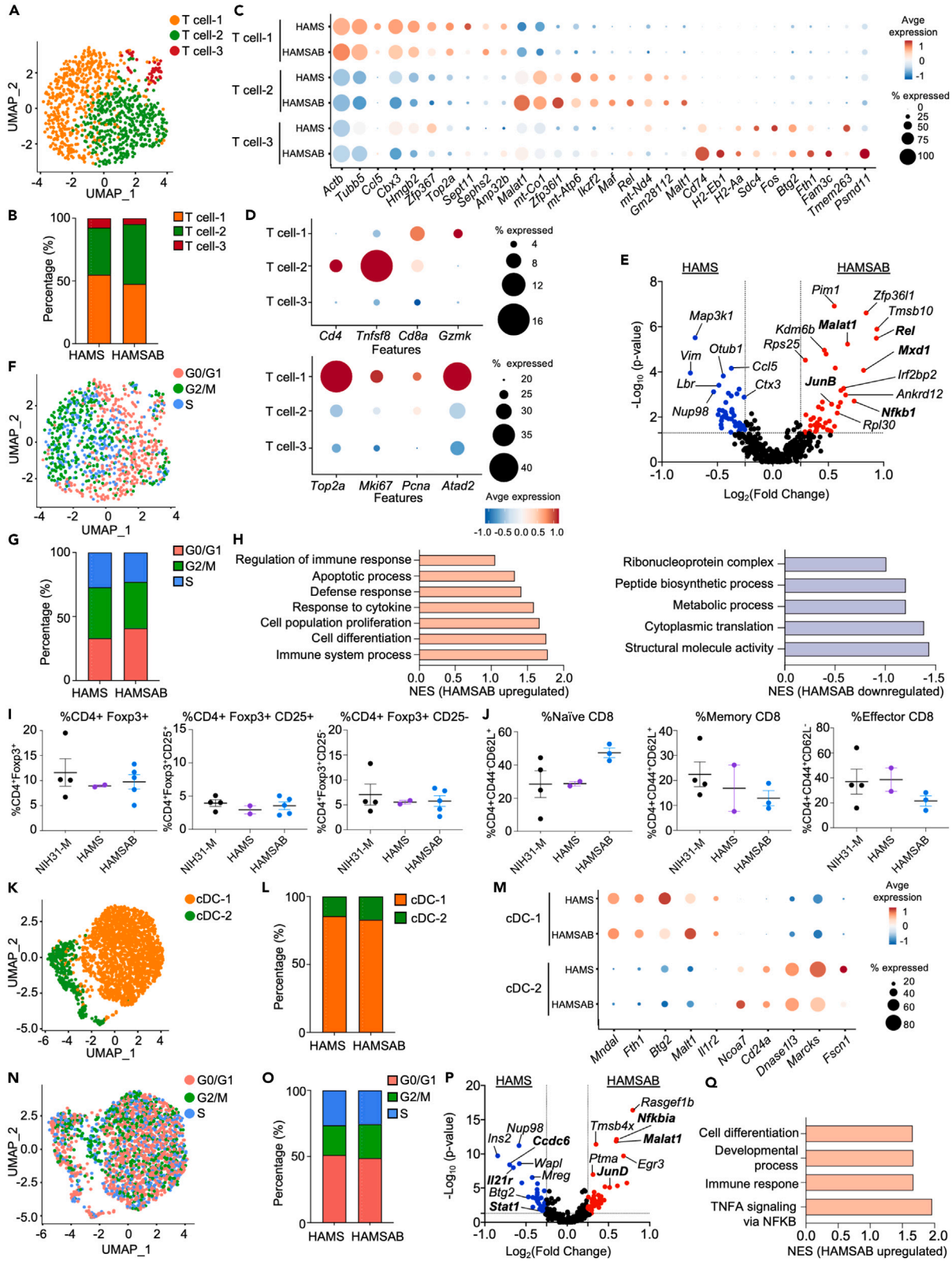
A
T cell-1
T cell-2
T cell-3
UMAP_2
UMAP_1
B
Percentage (%)
HAMS HAMSAB
C
HAMS
HAMSAB
Avge expression
% expressed
Actb Tubb5 Ccl5 Cbx3 Hmgb2 Zfp367 Top2a Sept11 Sephs2 Anp32b Malat1 mt-Co1 Zfp36l1 mt-Atp6 Ikzf2 Maf Rel mt-Nd4 Gm28112 Malt1 Cd74 H2-Eb1 H2-Aa Sdc4 Fos Btg2 Fth1 Fam3c Tmem263 Psmd11
D
Cd4 Tnfsf8 Cd8a Gzmk
Top2a Mki67 Pcna Atad2
Features
E
HAMS
HAMSAB
-Log10 (p-value)
Log2(Fold Change)
Pim1 Zfp36l1 Tmsb10 Map3k1 Kdm6b Malat1 Rel Rps25 Mxd1 Vim Otub1 Ccl5 Irf2bp2 Lbr Ctx3 JunB Ankrd12 Nup98 Nfkb1 Rpl30
F
G0/G1
G2/M
S
G
H
Regulation of immune response
Apoptotic process
Defense response
Response to cytokine
Cell population proliferation
Cell differentiation
Immune system process
NES (HAMSAB upregulated)
Ribonucleoprotein complex
Peptide biosynthetic process
Metabolic process
Cytoplasmic translation
Structural molecule activity
NES (HAMSAB downregulated)
I
%CD4+ Foxp3+
%CD4+ Foxp3+ CD25+
%CD4+ Foxp3+ CD25-
NIH31-M HAMS HAMSAB
J
%Naïve CD8
%Memory CD8
%Effector CD8
K
cDC-1
cDC-2
L
M
Mndal Fth1 Btg2 Malt1 Il1r2 Ncoa7 Cd24a Dnase1l3 Marcks Fscn1
N
O
P
Rasgef1b Nfkbia Nup98 Tmsb4x Malat1 Ins2 Ccdc6 Ptma Egr3 Wapl Mreg JunD Il21r Btg2 Stat1
Q
Cell differentiation
Developmental process
Immune respone
TNFA signaling via NFKB
NES (HAMSAB upregulated)

Figure 3. The HAMSAB diet induces a regulatory profile in T cells and cDCs in the pancreas of NOD mice

(A) UMAP dimension reduction analysis of T cells showing three populations.
(B) Bar chart indicating the percentage of the cells within the clusters in HAMSAB and HAMS islets.
(C) Top genes modulated in each cluster are indicated.
(D) Dot plot showing cell annotation of $CD4^+$ T cells (*Cd4*, *Tnfsf8*), $CD8^+$ T cells (*Cd8a*, *Klrc1*) and proliferation markers (*Top2a*, *Mki67*, *Pcna* and *Atad2*) in the different sets.
(E) Volcano plot of differentially expressed genes in T cells in HAMSAB and HAMS islets.
(F) UMAP of proliferating T cells.
(G) Fraction of proliferating T cells in HAMS and HAMSAB islets are shown in the bar chart.
(H) Upregulated and downregulated GSEA pathway analysis of the differentially expressed genes between HAMSAB and HAMS diet in T cells.
(I) Frequency of islet *Foxp3*$^+$$CD4^+$ T cells from 30-week-old female NOD mice fed HAMSAB, HAMS or NIH control diets.
(J) Frequency of islet Naive, Memory or Effector $CD8^+$ T cells from 30-week-old female NOD mice fed HAMSAB, HAMS or NIH control diets.
(K) Two sets were found for cDC shown in a UMAP dimension reduction analysis.
(L) Bar chart indicating the percentages of each cluster present in the different diets.
(M) Top genes for each cluster represented as dot plot. N. UMAP of proliferating cDC cells.
(O) Fraction of proliferating cDC cells in HAMS and HAMSAB islets are shown in the bar chart.
(P) Volcano plot of differentially expressed genes in cDCs in HAMSAB and HAMS islets.
(Q) GSEA analysis of differentially expressed genes in cDCs. Data are presented as mean ± standard error of the mean (SEM).

morphogenetic protein (BMP) signaling is upregulated in β cells by pro-inflammatory cytokines and negatively regulates β-cell function and growth.[22] In summary, from the early stage of the autoimmune process, islets harbor a range of various infiltrating immune cells, which can be affected by the administration of the HAMSAB dietary treatment.

Single-cell RNA sequencing analysis shows a regulatory immune cell profile in HAMSAB-fed NOD mice

Next, we performed unsupervised re-clustering and found three distinctive subpopulations of T cells from both groups: T cell-1, T cell-2 and T cell-3 (Figures 3A–3C, S2A, and S2B). HAMSAB islet cells showed a higher percentage of T cell-2 (47% for HAMSAB and 37% for HAMS), while in HAMS T cell-1 prevailed (47% for HAMSAB vs. 55% for HAMS) (Figure 3B). Gene annotation of T cell populations identified $CD4^+$ T cells mainly present in T cell-2 and $CD8^+$ T cells present in T cell-1 (Figures 3D and S2C). Gene expression analysis of T cells showed increased regulatory genes (*JunB, Rel, Nfkb1, Malat1*) in islets from HAMSAB-fed mice (Figure 3E). Additionally, T cell-1 presented higher proliferative signatures compared to T cell-2 and T cell-3 (S/G2/M phases, Figures 3F and 3G), which were predominant in islets from HAMS-fed mice (67% vs. 59% in HAMSAB islets).

We did not observe significant differences in $CD4^+$Foxp3$^+$ T cell frequencies in HAMSAB whole pancreas compared to controls, which was analyzed by FACS at the end of the observation period (30-week, Figure 3I). Thus, we investigated $CD4^+$ T cell subtypes and gene expression in infiltrated islets from the different diets. $CD4^+$ T cells were divided into four subpopulations (Figure S2D) expressing markers of different activation states (*Lef1*, *Ptma*, *Ccr7*, *Foxp3*, etc. Figure S2E). The regulatory population was mainly grouped in Cd4-2, expressing *Foxp3* and *Il10*, with a slightly higher percentage in HAMSAB-islets (30% vs. 27% in HAMS control, Figure S2F). In addition, proliferating $CD4^+$ T cells were mainly predominant in HAMS islets (Figures S2G–S2I). Analysis of $CD8^+$ T cells pooled from both diets revealed two distinctive subpopulations (Figure S3A). Cytotoxic *Gzma*$^+$ cells were found in Cd8-2 (Figure S3B). This subtype was lower in HAMSAB islets (37% vs. 63% in HAMS islets, Figure S3C). Interestingly, the trend was maintained 30 weeks after feeding, when islet immune cells were analyzed by FACS-sorting in NOD mice fed HAMSAB or control diets (Figure 3J). No differences were observed in $CD8^+$ T cell proliferation (Figures S3D–S3F). Pathway analysis performed on the differentially expressed T cell genes demonstrated a significant increase in regulation of immune response, apoptotic process, defense response, response to cytokines, transcription, mRNA, and translation in HAMSAB islets (Figures 3H and S4).

cDCs are indispensable for diabetes initiation, but also important for both central and peripheral tolerance.[23] cDCs were present as two major subpopulations (Figures 3K–3M and S5A–S5D), which were equally distributed in islets from HAMSAB- and HAMS-fed mice (Figure 3L). Proliferation of cDCs was not different between diets (Figures 3N and 3O). *Stat1*, a key IFN-γ–induced inflammatory marker,[24] was upregulated in islets from HAMS-fed mice (Figure 3P). On the other hand, the tolerogenic genes *Malat1*, *JunD* and *Nfkbia* were upregulated in islets from HAMSAB-fed mice (Figure 3P). Plasmacytoid dendritic cells (pDCs) were a minority of the cell population, allocated into two clusters (Figures S5E–S5J). Pathway analysis showed upregulation of cell differentiation, developmental process, immune response, translation, GTPase activator/regulator activity (cDC) and translation, and immune/cytokine receptor activity (pDC) among the differentially expressed genes in islets from HAMSAB- compared to HAMS-fed mice (Figures 3Q, S6, and S7).

We identified three subtypes of B cells with a similar percentage distribution in islets from both diets (Figures 4A–4D and S8A). *Pax5* and *Cxcr4* were upregulated in HAMSAB islets (Figures 4E and S8B). Cycling B cells represented half of the population and the percentages were not different between the two groups (Figures 4F and 4G). Pathway analysis showed peptide and amide metabolic process, (cytosolic) ribosome and structural molecular activity, RNA binding, protein containing complex organization and cell death, Th17/IL-17 signaling, type 1 diabetes, MHC class II protein complex binding in the differentially modified populations in HAMSAB and HAMS islets (Figures 4H and S8C).

Single-cell RNA sequencing analysis of macrophages revealed two distinct subpopulations in HAMSAB and HAMS islets: Mac-1 and Mac-2 (Figures 4I–4L and S9A). The inflammatory markers *Cxcl9, Sod2, Ccl5* and *Tapbp*, indicative of activated macrophages, were upregulated in Mac-1 (Figures 4K and S9B). HAMSAB had a higher percentage of this population (60% vs. 39% in HAMS islets, Figure 4J). On the other hand, Mac-2 was predominant in HAMS islets and contained MHC-I (*H2-M2, H2-K1*) and MHC-II (*H2-Eb1, H2-Aa, H2-D1*) molecules (Figure 4K). The

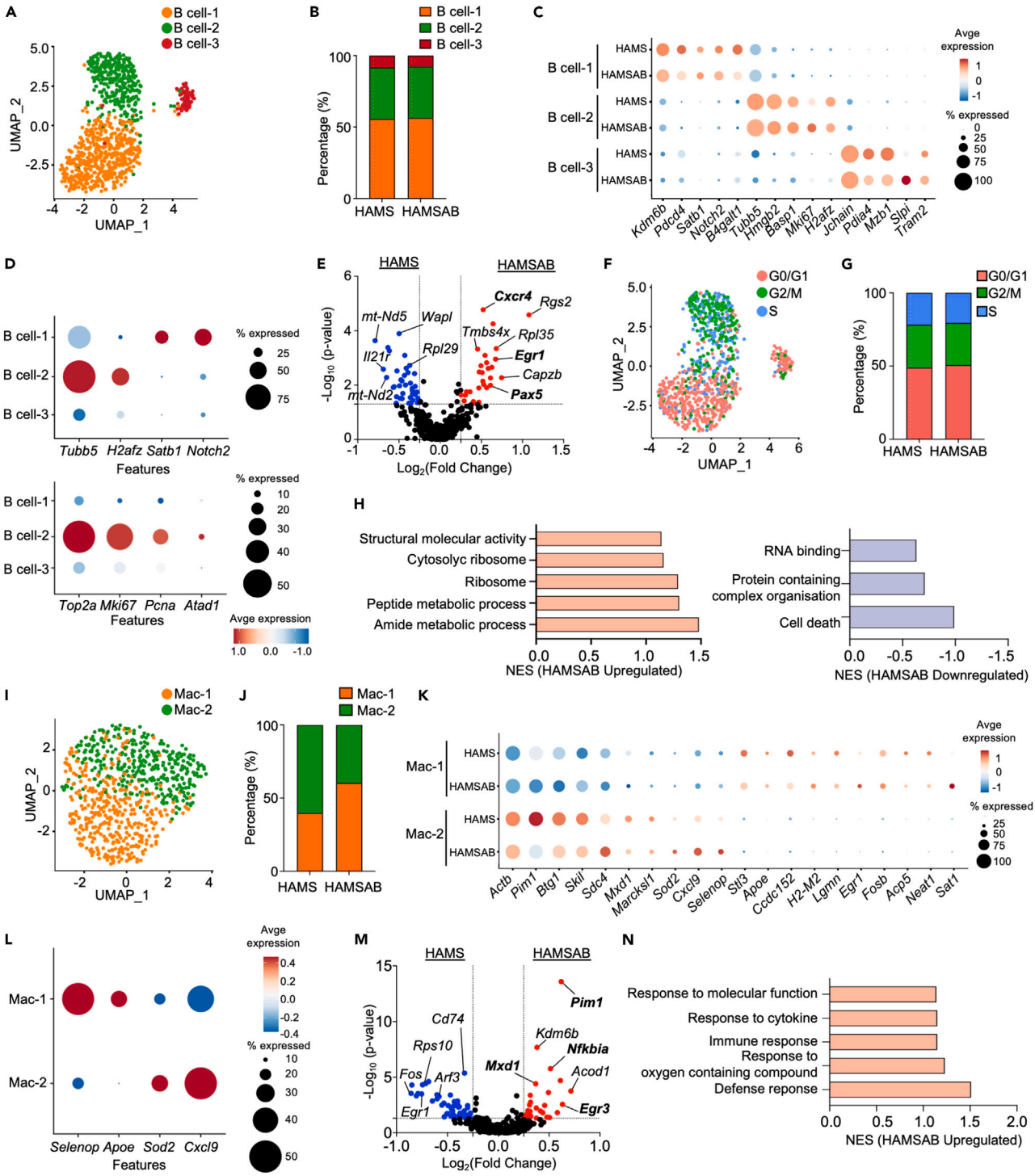

Figure 4. The HAMSAB diet affects gene transcription of B cells and macrophages in the pancreas of NOD mice

(A) Dimension reduction analysis of B cells showed three populations.

(B) There is no difference observed in the abundance of the subclusters compared in both diets.

(C) Top genes modulated in each cluster are indicated in a dot plot.

(D) Dot plot with markers genes for B cells (top) and proliferation markers (bottom) are shown in the different populations.

(E) Volcano plot of differentially expressed genes in B cells in HAMSAB and HAMS islets.

(F) UMAP of B cell proliferating cells.

Figure 4. *Continued*
(G) Fraction of proliferating B cells in HAMS and HAMSAB islets are shown in the bar chart.
(H) GSEA pathway analysis of the differentially expressed genes between HAMSAB and HAMS diet in B cells.
(I) Two main clusters are found in macrophages.
(J) Bar chart indicating the percentage of cells within the clusters in HAMSAB and HAMS islets.
(K) The top genes modulated in each cluster are indicated in a dot plot.
(L) Gene markers for macrophages in the UMAP graph.
(M) Volcano plot of differentially expressed genes in macrophages in HAMSAB and HAMS islets.
(N) GSEA pathway analysis of the differentially expressed genes between HAMSAB and HAMS diet in macrophages.

proliferation percentage of islet macrophages was similar between HAMSAB and HAMS islets (Figures S9C and S9D). *Pim1*, *Nfkbia*, *Mxd1* and *Egr3* were upregulated in HAMSAB islets, and *Fos*, *Egr1*, *Arf3* in HAMS islets (Figure 4M). Pathway analysis indicated response to molecular functions, response to cytokines, immune and defense response, Th17/IL-17 signaling, type 1 diabetes and MHC class II protein complex binding among the differentially modified clusters in HAMSAB and HAMS islets (Figures 4N and S9E).

Single-cell RNA sequencing analysis shows reduced stress markers and increased functional gene expression in endocrine cells of islets from HAMSAB-fed mice

Next, we focused our study on endocrine (β, α, δ, PP) cells. Pancreatic β cells presented two distinctive populations with no major differences in percentage between the two diet groups (Figures 5A–5C and S10A). Importantly, key functional β-cell genes (*Ins1*, *Iapp*, *G6pc2*, *Prlr*, *Ssr3*) were increased in islets from HAMSAB-fed mice (Figure 5D). Conversely, stress response genes (*Fos*, *Impact*, *Stat1*, *Dusp1*, *Hsp40/Dnajb1*) were upregulated in the HAMS islets (Figure 5D). In line with these findings, butyrate decreased cytokine-induced cell death in mouse primary islet cells (Figure 5E) and c-Fos and caspase-3 activation in INS-1E β cells (Figure 5F). Pathway analysis showed upregulated endoplasmic reticulum, signaling receptor binding, molecular function activator activity, hormone transport, Golgi-to-ER retrograde transport and unfolded protein binding among the differentially expressed genes between HAMSAB and HAMS islets (Figures 5G and 5H). These upregulated programs suggest that β cells have an increased function in HAMSAB islets.

We performed a Rank-Rank Hypergeometric Overlap (RRHO) analysis,[25] comparing ranked lists of genes identified by bulk RNA sequencing of primary β cells of T1D and control organ donors[26] and our dataset (Figure 5I). Key functional genes (*Ins*, *Iapp*, *Prlr*, *G6pc2*) were downregulated in HAMS/T1D compared to HAMSAB/control β cells (Figure 5J). In contrast, stressor genes (*Fos*, *Impact*) were upregulated in T1D/HAMS β cells (Figure 5J). Pathway analysis of these up- or downregulated genes indicated that autoimmunity activates programs of apoptosis, cellular responses to stress and induces dedifferentiation in β cells, which can be reduced by the HAMSAB diet (Figure 5K).

We performed differential expression analysis comparing gene expression in the α cells and found two sets (Figures 6A, 6B, and S10B). α cell-2, showing the endocrine progenitor marker *Mafa* and poly-hormonal (glucagon/insulin) cells, was mainly present in HAMS islets, but not in HAMSAB (Figure 6C). Moreover, functional α-cell genes (*Gcg*, *Gpx3*) were highly expressed in HAMSAB islets (Figure 6D). Confocal microscopy confirmed the presence of poly-hormonal cells in pancreatic islets from HAMS-fed mice (Figures 6E and S10C). Pathway analysis showed increased extracellular space, translation, and mRNA binding among the differentially expressed genes in HAMSAB compared to HAMS islets (Figure S11A). Negative regulation of gene expression, regulation of immune system process, regulation of cell differentiation, regulation of response stress are programs activated by autoimmunity that are decreased in α cells by the HAMSAB diet (Figure 6F).

δ cells were allocated in three different sets (Figures 6G, 6H, and S11B). Like α cells, δ cell-3 represented poly-hormonal (somatostatin/insulin) cells and endocrine progenitor makers (*Mafa*, *Nfix*), and was mainly present in HAMS islets (Figures 6I and 6J). Pathway analysis performed on differentially expressed genes between the two groups showed enrichment in translation and mRNA binding terms in δ cells in HAMSAB (Figures 6K and S11C). Similar results were observed in PP cells (Figures S12A–S12D). Interestingly, from the endocrine cells, only PP cells showed proliferation activity (Figure S12E). Enrichment in insulin secretion and hormone activity in PP cells was also found in HAMSAB islets compared to HAMS islets (Figure S12F). α, δ, and PP cells showed higher expression of polyhormonal (*Ins1*, *Ins2*) and stress genes (*Fos*) (Figures 6D, 6I, and S12D). Taken together, our data show an SCFA-dependent regulation of endocrine cell identity and function in autoimmune-mediated inflammation.

SCFAs improve differentiation of human embryonic stem cells into β-like cells

To test whether HAMSAB increases insulin expression, we exposed *in vitro* INS-1E cells to SCFAs. We observed that butyrate increased expression of β cell identity genes *Nkx6.1*, *Pdx1*, *Ins1* and *Ins2* (Figure 6L) and upregulated the SCFA receptors (Figure S13A) involved in insulin secretion.[27] Additionally, butyrate increased NKX6.1 expression (Figure 6M) and insulin levels (Figure 6N) in human embryonic stem cells (hESC)-differentiated β-like cells. We took advantage of the hESC model to study the effect of SCFAs in the differentiation transition to β-like cells. Analysis of single-cell RNA sequencing on the last stages of H1 differentiation in β-like cells[28] indicated that SCFA receptors were expressed in early β cells (stage 6) and had the highest expression in late β cells (stage 7) (Figure S13B). Thus, H1 hESCs were differentiated into pancreatic progenitors using a seven-stage protocol based on previously published reports,[29,30] with addition of acetate and butyrate from stage 6 (Figure S13C). Remarkably, SCFAs increased the number of insulin (but not glucagon) positive β-like cells (Figure 6O).

Few but functionally positive β-like cells can presumably impact circulating C-peptide levels. We transplanted hESC-derived endocrine aggregates into NOD/SCID female mice, which are devoid of T and B cells. At 14–16 weeks post transplantation, mice with low responder

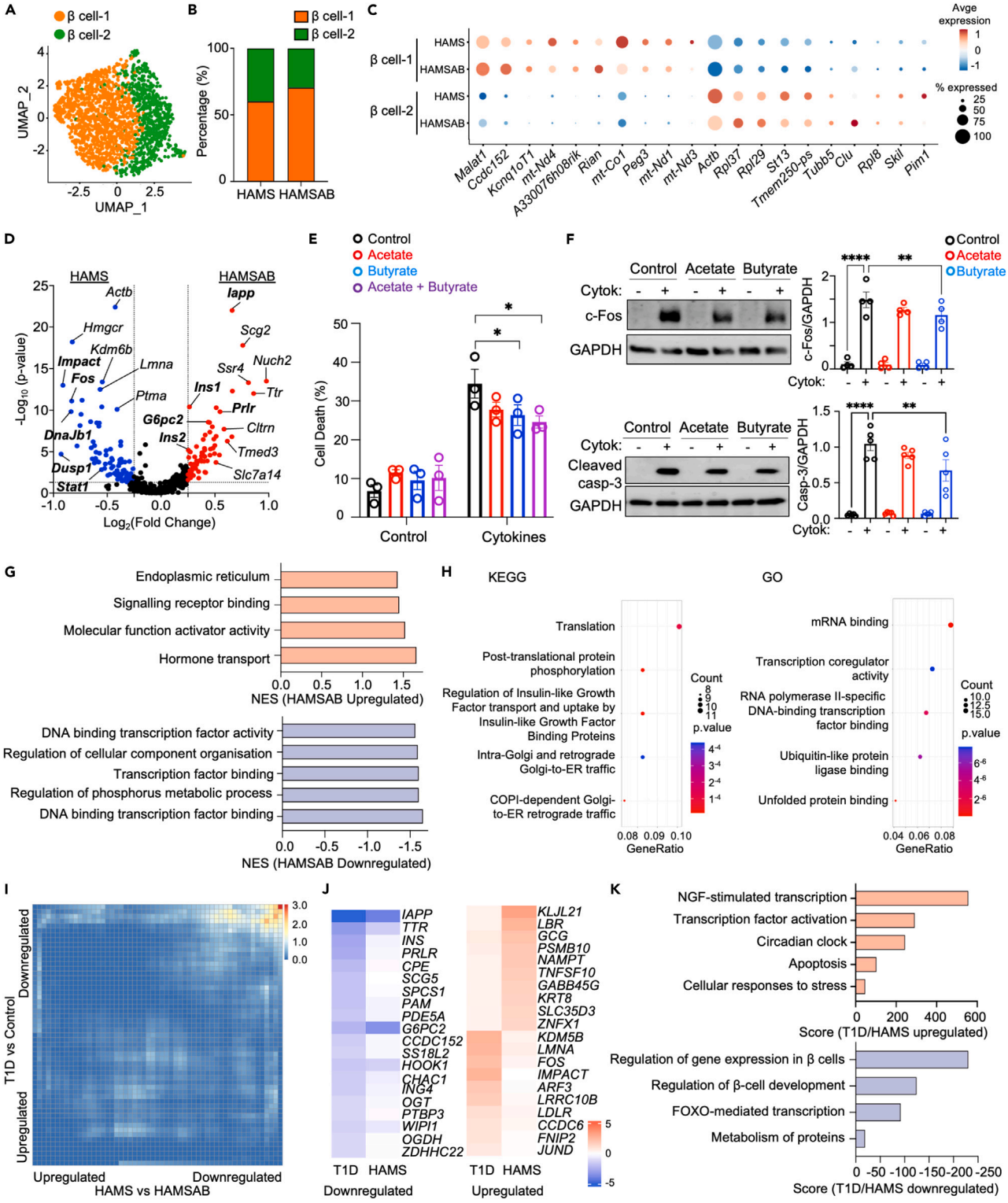

Figure 5. HAMSAB reduces β-cell stress makers and increases functional gene expression affected by autoimmunity development

(A) Dimension reduction analysis using UMAP clustering of β cells into two subclusters.

(B) Bar chart indicating the percentage of cells within the clusters in HAMSAB and HAMS islets.

(C) Dot plot indicating the gene expression levels within the distinct clusters in HAMSAB and HAMS islets.

(D) Volcano plot of differentially expressed genes in β cells in HAMSAB and HAMS islets.

Figure 5. *Continued*

(E) Cell death (%) of primary mouse islets after 24h exposure to pro-inflammatory cytokines, acetate (1mM) and/or butyrate (1mM) as indicated (n = 4).

(F) Western blot showing c-Fos (2h) and cleaved caspase-3 (24h) expression after cytokine exposure, in acetate (250μM) or butyrate (10μM) 24h pre-treated INS-1E cells (n = 4–5).

(G) GSEA pathway analysis of the differentially expressed genes between HAMSAB and HAMS diet in β cells.

(H) Top 5 of modified KEGG and GO pathways in HAMSAB and HAMS diet in β cells.

(I) RRHO analysis in HAMSAB/HAMS and T1D/control β cells.

(J) Top 10 downregulated and upregulated genes differentially expressed in T1D/HAMS compared to control/HAMSAB β cells.

(K) GSEA pathway analysis of all overlapping differentially expressed genes in T1D/HAMS compared to control/HAMSAB β cells. Data are presented as mean ± standard error of the mean (SEM). *p < 0.05, **p < 0.01, ***p < 0.001, ****p < 0.0001.

aggregates (human C-peptide<30 pmol/L) were treated with acetate and butyrate in drinking water. Human C-peptide was increased in the serum after 1 week of SCFA administration, suggesting graft improvement (Figure 6P).

DISCUSSION

Novel strategies are required to maintain islet β-cell survival and function after new-onset T1D.[1] A therapeutic diet can be a relevant and attractive approach to improve glucose homeostasis in the disease. HAMSAB releases large amounts of acetate and butyrate after bacterial fermentation in the colon.[6,8,31,32] We have recently shown that the HAMSAB supplement is safe and can improve glycemic control in T1D patients.[6]

In the present study, we demonstrated that HAMSAB impacts gene signatures related to infiltrated $CD4^+$, $CD8^+$ T cells, B cells, DCs and macrophages, consistent with our previous clinical trial in patients with established T1D.[6] Remarkably, changes in the composition and function of islet-infiltrated immune cells, following HAMSAB supplementation, resulted in a regulatory gene expression immune phenotype. In keeping with this, we observed reduced receptor-ligand expression in HAMSAB islets. This allows us to postulate reduced immune-endocrine cell interaction associated with immune-mediated β-cell dysfunction and death. Importantly, we found a correlation in gene expression in β cells related to dedifferentiation and stress in HAMS/HAMSAB and human T1D/control organ donors.[26]

HAMSAB administration decreased endocrine cell stress markers, which is consistent with previous observations.[14,33] The role of SCFA on β-cell identity in physiology/pathophysiology, however, is still controversial[34,35] and no studies have reported *in vivo* data with cell tracers. HAMSAB prevented the appearance of double hormonal endocrine cells in NOD mice (present data), also characteristic of type 1 diabetic patients.[36–38] This cell type may be derived from stressed β cells *trans*-differentiating into α cells.[39] This is proposed to be a β-cell survival mechanism to the inflammatory milieu. Yet, the functionality of these poly-hormonal cells is still unclear.[39] SCFA improved insulin levels in hESC-differentiated β-like cells *in vitro* in addition to human C-peptide levels when low responder aggregates were transplanted into NOD/SCID mice. These results may be relevant for boosting the residual β-cell mass in type 1 diabetic patients (fasting C-peptide<30 pmol/L), which can be found several years after diagnosis.[1,40]

In conclusion, we show that HAMSAB has an anti-inflammatory action in pancreatic islets in the context of autoimmune diabetes. HAMSAB clinical trials in children and adolescents with newly diagnosed T1D and hypertension have recently been launched in the US and Australia, respectively (ClinicalTrials.gov Identifier: NCT04114357 and Australia and New Zealand Clinical Trial Registry ACTRN12619000916145).[32,41] Our findings provide evidence of the mechanisms of action of SCFAs in different endocrine and immune cell populations, which support the use of HAMSAB for additional clinical studies in T1D.

Limitations of the study

A major concern is the reproducibility and translation of therapeutic approaches in preclinical models,[42–44] particularly therapeutics based on NOD mice.[43] In line with previous results,[8] we found reduced diabetes incidence after HAMSAB diet intervention in a small cohort of NOD mice used for the analysis. However, we did not observe complete diabetes protection. This is probably due to the higher diabetogenic backbone diet used in our NOD colony. In addition, we fed the mice for 5 weeks instead of the previous 10-week protocol,[8] to determine the preventive effects before diabetes onset (<12–15 weeks of age).

NOD mice start to show the peak expansion of autoreactive T and B cells consistent with the first signs of diabetes at approximately 12–15 weeks of age or onwards.[7,45,46] One caveat of our study is that single-cell RNA sequencing was performed at a very early stage of the disease in pooled islets from still normoglycemic mice (<200 mg/dL, 10 weeks of age). It is conceivable that some of these mice would not develop diabetes, adding variability to the cell population. Nonetheless, the aim of our study was to track the earliest changes after HAMSAB treatment ceased. HAMS control diet could delay the disease in ~21% in female NOD mice. This may be related to small traces of SCFAs coming from the fiber starch backbone, as has been shown in other studies with high fiber.[47] Further single-cell RNA sequencing of islets including different diets will add *in vivo* mechanistic insights. These studies will aid in assessing the relevance of the acetate or butyrate from HAMSAB, not only by comparison with the HAMS control diet. Moreover, it will be relevant to determine whether HAMSAB provides similar protection regardless of when or for how long the diet is administered.

STAR★METHODS

Detailed methods are provided in the online version of this paper and include the following:

- KEY RESOURCES TABLE

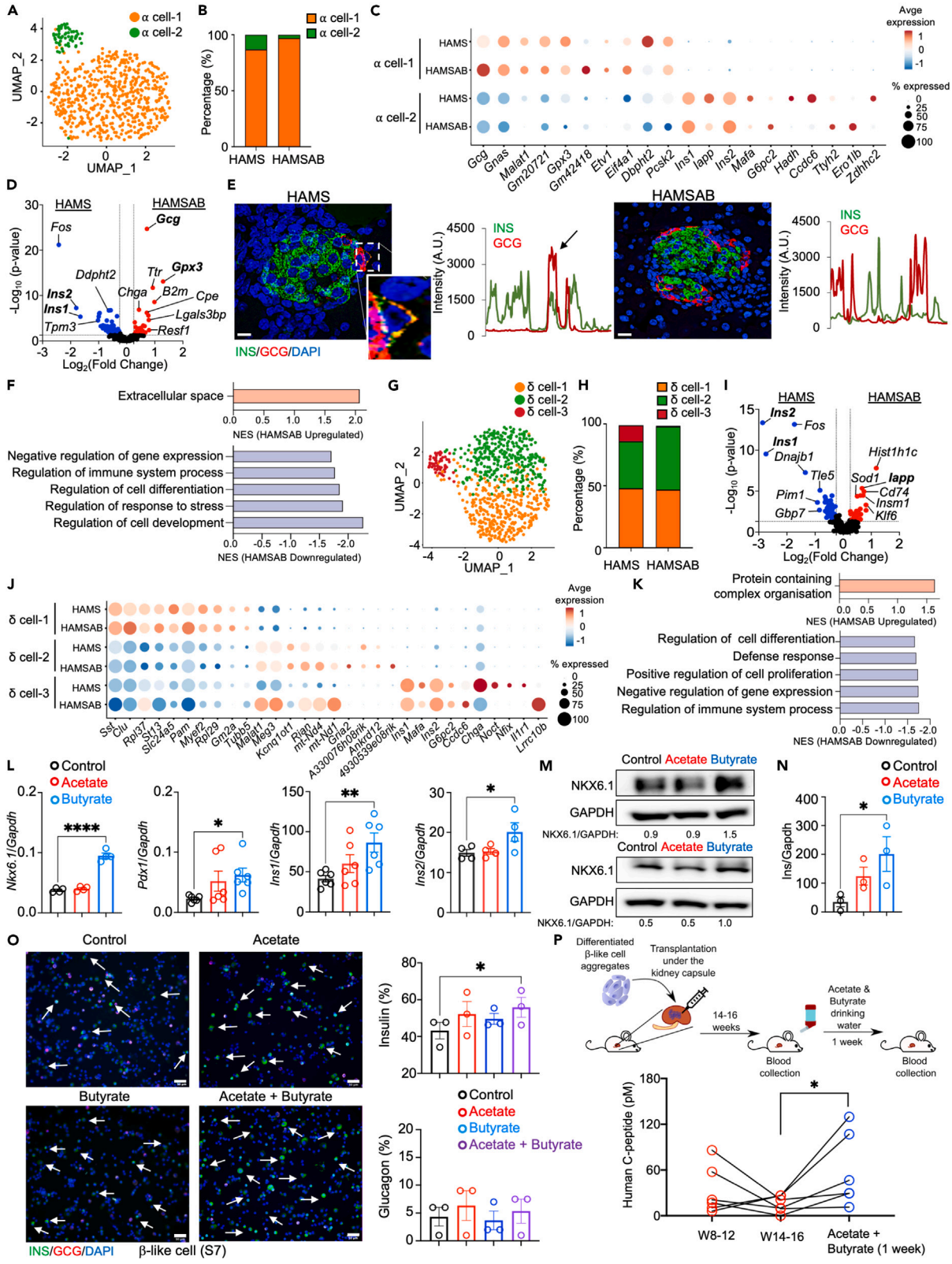
A
α cell-1
α cell-2
UMAP_2
UMAP_1
B
α cell-1
α cell-2
Percentage (%)
HAMS HAMSAB
C
Avge expression
% expressed
α cell-1
α cell-2
HAMS
HAMSAB
Gcg Gnas Malat1 Gm20721 Gpx3 Gm42418 Etv1 Eif4a1 Dbpht2 Pcsk2 Ins1 Iapp Ins2 Mafa G6pc2 Hadh Ccdc6 Ttyh2 Ero1lb Zdhhc2
D
HAMS
HAMSAB
-Log10 (p-value)
Log2(Fold Change)
Fos
Gcg
Ddpht2
Ttr
Gpx3
Ins2
Ins1
Chga
B2m
Cpe
Lgals3bp
Tpm3
Resf1
E
HAMS
HAMSAB
INS/GCG/DAPI
INS
GCG
Intensity (A.U.)
F
Extracellular space
NES (HAMSAB Upregulated)
Negative regulation of gene expression
Regulation of immune system process
Regulation of cell differentiation
Regulation of response to stress
Regulation of cell development
NES (HAMSAB Downregulated)
G
δ cell-1
δ cell-2
δ cell-3
UMAP_2
UMAP_1
H
δ cell-1
δ cell-2
δ cell-3
Percentage (%)
HAMS HAMSAB
I
HAMS
HAMSAB
Ins2
Fos
Ins1
Dnajb1
Hist1h1c
Tle5
Sod1
Iapp
Cd74
Pim1
Insm1
Gbp7
Klf6
-Log10 (p-value)
Log2(Fold Change)
J
Avge expression
% expressed
δ cell-1
δ cell-2
δ cell-3
HAMS
HAMSAB
Sst Clu Rpl37 Slf13 Slc24a5 Pam Myef2 Rpl29 Gm2a Tubb5 Malat1 Meg3 Kcnq1ot1 Riap mt-Nd4 mt-Nd1 Gria2 A330076h08rik Ankrd12 4930539e08rik Ins1 Mafa Ins2 G6pc2 Ccdc6 Chga Nocl Nfix Irr1 Lrrc10b
K
Protein containing complex organisation
NES (HAMSAB Upregulated)
Regulation of cell differentiation
Defense response
Positive regulation of cell proliferation
Negative regulation of gene expression
Regulation of immune system process
NES (HAMSAB Downregulated)
L
Control
Acetate
Butyrate
Nkx6.1/Gapdh
Pdx1/Gapdh
Ins1/Gapdh
Ins2/Gapdh
M
Control Acetate Butyrate
NKX6.1
GAPDH
NKX6.1/GAPDH: 0.9 0.9 1.5
Control Acetate Butyrate
NKX6.1
GAPDH
NKX6.1/GAPDH: 0.5 0.5 1.0
N
Control
Acetate
Butyrate
Ins/Gapdh
O
Control
Acetate
Butyrate
Acetate + Butyrate
INS/GCG/DAPI
β-like cell (S7)
Insulin (%)
Glucagon (%)
Control
Acetate
Butyrate
Acetate + Butyrate
P
Differentiated β-like cell aggregates
Transplantation under the kidney capsule
14-16 weeks
Blood collection
Acetate & Butyrate drinking water
1 week
Blood collection
Human C-peptide (pM)
W8-12
W14-16
Acetate + Butyrate (1 week)

Figure 6. Single-cell RNA sequencing analysis shows endocrine cell identity preservation in HAMSAB islets and SCFA increase insulin levels in hESC-differentiated β-like cells

(A) Dimension reduction by UMAP of α cells.
(B) Bar chart indicating the percentage of cells within populations in HAMSAB and HAMS islets.
(C) Dot plot showing the highest modified genes for both subtypes.
(D) Volcano plot of differentially expressed genes in α cells in HAMSAB and HAMS islets.
(E) Confocal images of the pancreas from NOD mice fed with HAMS or HAMSAB diets. Scale bar: 10μm.
(F) GSEA pathway analysis of the differentially expressed genes between HAMSAB and HAMS diet in α cells.
(G) UMAP populations of δ cells.
(H) Bar chart indicating the percentage of cells within the subtypes in HAMSAB and HAMS islets.
(I) Volcano plot of differentially expressed genes in δ cells in HAMSAB and HAMS islets.
(J) Dot plot showing the highest modified genes for both subtypes.
(K) GSEA pathway analysis of the differentially expressed genes between HAMSAB and HAMS diet in δ cells.
(L) qPCR analysis of *Nkx6.1*, *Pdx1*, *Ins1* and *Ins2* gene expression in INS-1E cells treated with acetate (1mM) or butyrate (1mM) for 24h. *Gapdh* was used as housekeeping gene (n = 4–6).
(M) hESC-derived aggregates were cultured with acetate (1mM) or butyrate (1mM) for 24h. Western blot was performed and the relative protein expression of the NKX6.1 shown was quantified by dividing the intensity values against GAPDH as an internal housekeeping protein using ImageJ software (n = 2).
(N) Insulin expression in hESC-differentiated β-like cells treated with acetate (1mM) or butyrate (1mM) for 24h (n = 3).
(O) β-like cells were dispersed and fixed to measure % of positive insulin (white arrows) or glucagon cells by immunofluorescence (n = 3). Scale bar: 50μm.
(P) hESC-derived aggregates were transplanted into NOD/SCID mice as indicated. Low responder transplants were selected, and blood was collected from the tail at 8–12, and 14–16 weeks before and after 1 week addition of acetate (200mM) and butyrate (150mM) in the drinking water. Human C-peptide values were measured by ELISA (n = 6). Data are presented as mean ± standard error of the mean (SEM). *p < 0.05, **p < 0.01, ***p < 0.001, ****p < 0.0001.

SUPPLEMENTAL INFORMATION

Supplemental information can be found online at https://doi.org/10.1016/j.isci.2023.108694.

ACKNOWLEDGMENTS

We thank Madalina Popa, André Dias, Erick Arroba, Mariana Nunes, Francisco Costa, Anaïs Schaschkow (Université libre de Bruxelles) and Marijke Viaene (CEE, KU Leuven, Leuven, Belgium) for experimental and technical support, Stephanie Talamantes (Université libre de Bruxelles) for help with editing of the manuscript, and Eduardo Gilglioni for the design of the graphical abstract. The authors declare no conflict of interest. This work was supported by a European Research Council (ERC) Consolidator grant METAPTPs (GA817940), a JDRF Career Development Award (CDA-2019-758-A-N), and a Fonds National de la Recherche Scientifique (FNRS) CDR grant (40013655). V.V. is supported by an FNRS PhD Aspirant scholarship. S.P.S. is supported by MISU funding from the FNRS (34772792 – SCHISM). Work in the AKC group was supported by FNRS Excellence of Science grant (EOS 30826052) and research credit (CDR J.0109.220). P.X. is recipient of Fond David et Alice Van Buuren, Belgium. E.N.G. is a Research Associate of the FNRS, Belgium.

AUTHOR CONTRIBUTIONS

V.V., S.E.E., M.K.B., A.L., S.D., P.X., and A.K.C. research data and reviewed and edited the manuscript. N.B., L.G.M., and S.P.S. contributed to data analysis and reviewed and edited the manuscript. E.M. and C.G. contributed to research data, experimental design and reviewed and edited the manuscript. E.N.G. researched data; contributed to designed experiments; and reviewed, edited, and wrote the manuscript. E.N.G. is the guarantor of this work and, as such, has full access to all the data in the study and takes responsibility for the integrity of the data and the accuracy of the data analysis.

DECLARATION OF INTERESTS

E.M. is an inventor on a patent WO2018027274A1 submitted by Monash University that covers methods and compositions of metabolites for treatment and prevention of autoimmune disease related to this paper and stock ownership for ImmunoBiota Therapeutics Pty Ltd. E.N.G. declares that there are no other relationships or activities that might bias, or be perceived to bias, the present work.

Received: April 17, 2023
Revised: October 23, 2023
Accepted: December 5, 2023
Published: December 10, 2023

REFERENCES

1. Gurzov, E.N., Ke, P.C., Ahlgren, U., Garcia Ribeiro, R.S., and Gotthardt, M. (2020). Novel Strategies to Protect and Visualize Pancreatic beta Cells in Diabetes. Trends Endocrinol. Metabol. *31*, 905–917.
2. Richards, J.L., Yap, Y.A., McLeod, K.H., Mackay, C.R., and Mariño, E. (2016). Dietary metabolites and the gut microbiota: an alternative approach to control inflammatory and autoimmune diseases. Clin. Transl. Immunol. *5*, e82.
3. Sanna, S., van Zuydam, N.R., Mahajan, A., Kurilshikov, A., Vich Vila, A., Võsa, U., Mujagic, Z., Masclee, A.A.M., Jonkers, D.M.A.E., Oosting, M., et al. (2019). Causal relationships among the gut microbiome, short-chain fatty acids and metabolic diseases. Nat. Genet. *51*, 600–605.
4. Zhou, W., Sailani, M.R., Contrepois, K., Zhou, Y., Ahadi, S., Leopold, S.R., Zhang, M.J., Rao, V., Avina, M., Mishra, T., et al. (2019). Longitudinal multi-omics of host-microbe dynamics in prediabetes. Nature *569*, 663–671.
5. Vatanen, T., Franzosa, E.A., Schwager, R., Tripathi, S., Arthur, T.D., Vehik, K., Lernmark, Å., Hagopian, W.A., Rewers, M.J., She, J.X., et al. (2018). The human gut microbiome in early-onset type 1 diabetes from the TEDDY study. Nature *562*, 589–594.
6. Bell, K.J., Saad, S., Tillett, B.J., McGuire, H.M., Bordbar, S., Yap, Y.A., Nguyen, L.T., Wilkins, M.R., Corley, S., Brodie, S., et al. (2022). Metabolite-based dietary supplementation in human type 1 diabetes is associated with microbiota and immune modulation. Microbiome *10*, 9.
7. Mariño, E., Villanueva, J., Walters, S., Liuwantara, D., Mackay, F., and Grey, S.T. (2009). CD4(+)CD25(+) T-cells control autoimmunity in the absence of B-cells. Diabetes *58*, 1568–1577.
8. Mariño, E., Richards, J.L., McLeod, K.H., Stanley, D., Yap, Y.A., Knight, J., McKenzie, C., Kranich, J., Oliveira, A.C., Rossello, F.J., et al. (2017). Gut microbial metabolites limit the frequency of autoimmune T cells and protect against type 1 diabetes. Nat. Immunol. *18*, 552–562.
9. Tilg, H., Zmora, N., Adolph, T.E., and Elinav, E. (2020). The intestinal microbiota fuelling metabolic inflammation. Nat. Rev. Immunol. *20*, 40–54.
10. Spivak, I., Fluhr, L., and Elinav, E. (2022). Local and systemic effects of microbiome-derived metabolites. EMBO Rep. *23*, e55664.
11. Wen, L., and Wong, F.S. (2017). Dietary short-chain fatty acids protect against type 1 diabetes. Nat. Immunol. *18*, 484–486.
12. Snelson, M., Rampanelli, E., Nieuwdorp, M., Hanssen, N.M., and Coughlan, M.T. (2022). Microbial influencers: treating diabetes through the gut. Immunol. Cell Biol. *100*, 390–393.
13. Powers, A.C., Philippe, J., Hermann, H., and Habener, J.F. (1988). Sodium butyrate increases glucagon and insulin gene expression by recruiting immunocytochemically negative cells to produce hormone. Diabetes *37*, 1405–1410.
14. Hu, S., Kuwabara, R., de Haan, B.J., Smink, A.M., and de Vos, P. (2020). Acetate and Butyrate Improve beta-cell Metabolism and Mitochondrial Respiration under Oxidative Stress. Int. J. Mol. Sci. *21*, 1542.
15. Zhang, Y., Lei, Y., Honarpisheh, M., Kemter, E., Wolf, E., and Seissler, J. (2021). Butyrate and Class I Histone Deacetylase Inhibitors Promote Differentiation of Neonatal Porcine Islet Cells into Beta Cells. Cells *10*.
16. Pedersen, S.S., Prause, M., Williams, K., Barrès, R., and Billestrup, N. (2022). Butyrate inhibits IL-1beta-induced inflammatory gene expression by suppression of NF-kappaB activity in pancreatic beta cells. J. Biol. Chem. *298*, 102312.
17. Jansen, A., Homo-Delarche, F., Hooijkaas, H., Leenen, P.J., Dardenne, M., and Drexhage, H.A. (1994). Immunohistochemical characterization of monocytes-macrophages and dendritic cells involved in the initiation of the insulitis and beta-cell destruction in NOD mice. Diabetes *43*, 667–675.
18. Zakharov, P.N., Hu, H., Wan, X., and Unanue, E.R. (2020). Single-cell RNA sequencing of murine islets shows high cellular complexity at all stages of autoimmune diabetes. J. Exp. Med. *217*, e20192362.
19. Efremova, M., Vento-Tormo, M., Teichmann, S.A., and Vento-Tormo, R. (2020). CellPhoneDB: inferring cell-cell communication from combined expression of multi-subunit ligand-receptor complexes. Nat. Protoc. *15*, 1484–1506.
20. Martínez, A., Weaver, C., López, J., Bhathena, S.J., Elsasser, T.H., Miller, M.J., Moody, T.W., Unsworth, E.J., and Cuttitta, F. (1996). Regulation of insulin secretion and blood glucose metabolism by adrenomedullin. Endocrinology *137*, 2626–2632.
21. Dong, Y., Ruano, S.H., Mishra, A., Pennington, K.A., and Yallampalli, C. (2022). Adrenomedullin and its receptors are expressed in mouse pancreatic beta-cells and suppresses insulin synthesis and secretion. PLoS One *17*, e0265890.
22. Bruun, C., Christensen, G.L., Jacobsen, M.L.B., Kanstrup, M.B., Jensen, P.R., Fjordvang, H., Mandrup-Poulsen, T., and Billestrup, N. (2014). Inhibition of beta cell growth and function by bone morphogenetic proteins. Diabetologia *57*, 2546–2554.
23. Morel, P.A. (2013). Dendritic cell subsets in type 1 diabetes: friend or foe? Front. Immunol. *4*, 415.
24. Gurzov, E.N., Stanley, W.J., Pappas, E.G., Thomas, H.E., and Gough, D.J. (2016). The JAK/STAT pathway in obesity and diabetes. FEBS J. *283*, 3002–3015.
25. Plaisier, S.B., Taschereau, R., Wong, J.A., and Graeber, T.G. (2010). Rank-rank hypergeometric overlap: identification of statistically significant overlap between gene-expression signatures. Nucleic Acids Res. *38*, e169.
26. Russell, M.A., Redick, S.D., Blodgett, D.M., Richardson, S.J., Leete, P., Krogvold, L., Dahl-Jørgensen, K., Bottino, R., Brissova, M., Spaeth, J.M., et al. (2019). HLA Class II Antigen Processing and Presentation Pathway Components Demonstrated by Transcriptome and Protein Analyses of Islet beta-Cells From Donors With Type 1 Diabetes. Diabetes *68*, 988–1001.
27. Priyadarshini, M., Wicksteed, B., Schiltz, G.E., Gilchrist, A., and Layden, B.T. (2016). SCFA Receptors in Pancreatic beta Cells: Novel Diabetes Targets? Trends Endocrinol. Metabol. *27*, 653–664.
28. Balboa, D., Barsby, T., Lithovius, V., Saarimäki-Vire, J., Omar-Hmeadi, M., Dyachok, O., Montaser, H., Lund, P.E., Yang, M., Ibrahim, H., et al. (2022). Functional, metabolic and transcriptional maturation of human pancreatic islets derived from stem cells. Nat. Biotechnol. *40*, 1042–1055.
29. Elvira, B., Vandenbempt, V., Bauzá-Martinez, J., Crutzen, R., Negueruela, J., Ibrahim, H., Winder, M.L., Brahma, M.K., Vekeriotaite, B., Martens, P.J., et al. (2022). PTPN2 Regulates the Interferon Signaling and Endoplasmic Reticulum Stress Response in Pancreatic beta-Cells in Autoimmune Diabetes. Diabetes *71*, 653–668.
30. Schaschkow, A., Pang, L., Vandenbempt, V., Elvira, B., Litwak, S.A., Vekeriotaite, B., Maillard, E., Vermeersch, M., Paula, F.M.M., Pinget, M., et al. (2021). STAT3 Regulates Mitochondrial Gene Expression in Pancreatic beta-Cells and Its Deficiency Induces Glucose Intolerance in Obesity. Diabetes *70*, 2026–2041.
31. Yap, Y.A., McLeod, K.H., McKenzie, C.I., Gavin, P.G., Davalos-Salas, M., Richards, J.L., Moore, R.J., Lockett, T.J., Clarke, J.M., Eng, V.V., et al. (2021). An acetate-yielding diet imprints an immune and anti-microbial programme against enteric infection. Clin. Transl. Immunol. *10*, e1233.
32. Rhys-Jones, D., Climie, R.E., Gill, P.A., Jama, H.A., Head, G.A., Gibson, P.R., Kaye, D.M., Muir, J.G., and Marques, F.Z. (2021). Microbial Interventions to Control and Reduce Blood Pressure in Australia

(MICRoBIA): rationale and design of a double-blinded randomised cross-over placebo controlled trial. Trials *22*, 496.

33. Pingitore, A., Gonzalez-Abuin, N., Ruz-Maldonado, I., Huang, G.C., Frost, G., and Persaud, S.J. (2019). Short chain fatty acids stimulate insulin secretion and reduce apoptosis in mouse and human islets *in vitro*: Role of free fatty acid receptor 2. Diabetes Obes. Metabol. *21*, 330–339.
34. Wang, S., Yuan, M., Zhang, L., Zhu, K., Sheng, C., Zhou, F., Xu, Z., Liu, Q., Liu, Y., Lu, J., et al. (2022). Sodium butyrate potentiates insulin secretion from rat islets at the expense of compromised expression of beta cell identity genes. Cell Death Dis. *13*, 67.
35. Prause, M., Pedersen, S.S., Tsonkova, V., Qiao, M., and Billestrup, N. (2021). Butyrate Protects Pancreatic Beta Cells from Cytokine-Induced Dysfunction. Int. J. Mol. Sci. *22*, 10427.
36. Piran, R., Lee, S.H., Li, C.R., Charbono, A., Bradley, L.M., and Levine, F. (2014). Pharmacological induction of pancreatic islet cell transdifferentiation: relevance to type I diabetes. Cell Death Dis. *5*, e1357.
37. Chakravarthy, H., Gu, X., Enge, M., Dai, X., Wang, Y., Damond, N., Downie, C., Liu, K., Wang, J., Xing, Y., et al. (2017). Converting Adult Pancreatic Islet alpha Cells into beta Cells by Targeting Both Dnmt1 and Arx. Cell Metabol. *25*, 622–634.
38. Lam, C.J., Chatterjee, A., Shen, E., Cox, A.R., and Kushner, J.A. (2019). Low-Level Insulin Content Within Abundant Non-beta Islet Endocrine Cells in Long-standing Type 1 Diabetes. Diabetes *68*, 598–608.
39. Tesi, M., Bugliani, M., Ferri, G., Suleiman, M., De Luca, C., Bosi, E., Masini, M., De Tata, V., Gysemans, C., Cardarelli, F., et al. (2021). Pro-Inflammatory Cytokines Induce Insulin and Glucagon Double Positive Human Islet Cells That Are Resistant to Apoptosis. Biomolecules *11*, 320.
40. Oram, R.A., Sims, E.K., and Evans-Molina, C. (2019). Beta cells in type 1 diabetes: mass and function; sleeping or dead? Diabetologia *62*, 567–577.
41. Ismail, H.M., Spall, M., Evans-Molina, C., and DiMeglio, L.A. (2020). Evaluating the Effect of Prebiotics on the Gut Microbiome Profile and β-cell Function in Youth with Newly-Diagnosed Type 1 Diabetes. Preprint at medRxiv. https://doi.org/10.1101/2020.10.05.20207142.
42. Landis, S.C., Amara, S.G., Asadullah, K., Austin, C.P., Blumenstein, R., Bradley, E.W., Crystal, R.G., Darnell, R.B., Ferrante, R.J., Fillit, H., et al. (2012). A call for transparent reporting to optimize the predictive value of preclinical research. Nature *490*, 187–191.
43. Gill, R.G., Pagni, P.P., Kupfer, T., Wasserfall, C.H., Deng, S., Posgai, A., Manenkova, Y., Bel Hani, A., Straub, L., Bernstein, P., et al. (2016). A Preclinical Consortium Approach for Assessing the Efficacy of Combined Anti-CD3 Plus IL-1 Blockade in Reversing New-Onset Autoimmune Diabetes in NOD Mice. Diabetes *65*, 1310–1316.
44. Atkinson, M.A. (2011). Evaluating preclinical efficacy. Sci. Transl. Med. *3*, 96cm22.
45. Mariño, E., Batten, M., Groom, J., Walters, S., Liuwantara, D., Mackay, F., and Grey, S.T. (2008). Marginal-zone B-cells of nonobese diabetic mice expand with diabetes onset, invade the pancreatic lymph nodes, and present autoantigen to diabetogenic T-cells. Diabetes *57*, 395–404.
46. Mariño, E., Tan, B., Binge, L., Mackay, C.R., and Grey, S.T. (2012). B-cell cross-presentation of autologous antigen precipitates diabetes. Diabetes *61*, 2893–2905.
47. Ho, J., Nicolucci, A.C., Virtanen, H., Schick, A., Meddings, J., Reimer, R.A., and Huang, C. (2019). Effect of Prebiotic on Microbiota, Intestinal Permeability, and Glycemic Control in Children With Type 1 Diabetes. J. Clin. Endocrinol. Metab. *104*, 4427–4440.
48. Mathieu, C., Laureys, J., Sobis, H., Vandeputte, M., Waer, M., and Bouillon, R. (1992). 1,25-Dihydroxyvitamin D3 prevents insulitis in NOD mice. Diabetes *41*, 1491–1495.
49. Gurzov, E.N., Barthson, J., Marhfour, I., Ortis, F., Naamane, N., Igoillo-Esteve, M., Gysemans, C., Mathieu, C., Kitajima, S., Marchetti, P., et al. (2012). Pancreatic beta-cells activate a JunB/ATF3-dependent survival pathway during inflammation. Oncogene *31*, 1723–1732.
50. Hao, Y., Hao, S., Andersen-Nissen, E., Mauck, W.M., 3rd, Zheng, S., Butler, A., Lee, M.J., Wilk, A.J., Darby, C., Zager, M., et al. (2021). Integrated analysis of multimodal single-cell data. Cell *184*, 3573–3587.e29.
51. Hafemeister, C., and Satija, R. (2019). Normalization and variance stabilization of single-cell RNA-seq data using regularized negative binomial regression. Genome Biol. *20*, 296.
52. Stuart, T., Butler, A., Hoffman, P., Hafemeister, C., Papalexi, E., Mauck, W.M., 3rd, Hao, Y., Stoeckius, M., Smibert, P., and Satija, R. (2019). Comprehensive Integration of Single-Cell Data. Cell *177*, 1888–1902.e21.
53. Takiishi, T., Korf, H., Van Belle, T.L., Robert, S., Grieco, F.A., Caluwaerts, S., Galleri, L., Spagnuolo, I., Steidler, L., Van Huynegem, K., et al. (2012). Reversal of autoimmune diabetes by restoration of antigen-specific tolerance using genetically modified Lactococcus lactis in mice. J. Clin. Invest. *122*, 1717–1725.

STAR★METHODS

KEY RESOURCES TABLE

REAGENT or RESOURCE	SOURCE	IDENTIFIER
Antibodies		
Anti-c-Fos antibody	Cell Signaling	Cat# 4384, RRID:AB_2106617
Anti-Cleaved caspase-3 antibody	Cell Signaling	Cat# 9664 RRID:AB_2070042
Anti-NKX6.1 antibody	BD biosciences	Cat# 563022 RRID:AB_2737958
Anti-GAPDH antibody	Trevigen	Cat# 2275-PC-100
Anti-Rabbit IgG HRP	Dako	Cat# P0448
Anti-Mouse IgG HRP	Dako	Cat# P0447
Anti-Insulin antibody (cells)	Dako	Cat# IR002
Anti-Insulin antibody (pancreas slides)	Dako	Cat# A0564
Anti-Glucagon antibody	Sigma-Aldrich	Cat# G2654 RRID:AB_259852
Anti-Guinea pig-Alexa 488	Thermo Fisher	Cat# A11073 RRID:AB_2534117
Anti-Mouse-Alexa 555	Thermo Fisher	Cat# A32773 RRID:AB_2762848
Anti-CD3	Thermo Fisher	Cat# 145-2C11
Anti-CD4	Thermo Fisher	Cat# GK1.5
Anti-CD8a	Thermo Fisher	Cat# 53-6.7
Anti-CD25	Thermo Fisher	Cat# PC61.5
Anti-FoxP3	Thermo Fisher	Cat# FJK-16s
Anti-CD44	Thermo Fisher	Cat# IM7
Anti-CD26L	Thermo Fisher	Cat# MEL-14
Chemicals, peptides, and recombinant proteins		
Sodium Acetate	Sigma-Aldrich	Cat# S5636
Sodium Butyrate	Sigma-Aldrich	Cat# 303410
Mouse interferon-γ	PeproTech	Cat# 315-05
Human Interleukin-1β	R&D Systems	Cat# 201-LB
Rat Interferon-γ	R&D Systems	Cat# 585-IF
Trypsin	Sigma-Aldrich	Cat# T9935
DNAseI	Qiagen	Cat# 79254
Western blot cell lysis buffer	Cell Signaling	Cat# 9803S
Essential 8™ Medium	Gibco	Cat# A1517001
Matrigel	Corning	Cat# 356231
Collagenase	Sigma-Aldrich	Cat# C2674-1G
Critical commercial assays		
Chromium Next GEM Single Cell 3′ Reagent Kits v3.1	10X Genomics	Cat# PN-1000121
SYTOX Green Nucleid Acid Stain	Thermo Scientific	Cat# S7020
Human Ultra sensitive C-peptide ELISA	Mercodia	Cat# 10-1141-01
Propidium Iodide	Sigma-Aldrich	Cat# P4170
VECTASHIELD Antifade Mounting Medium with DAPI	Vector Laboratories	Cat# H-1200
MycoAlert Mycoplasma Detection Kit	Lonza	Cat# LT07-218

(*Continued on next page*)

Continued

REAGENT or RESOURCE	SOURCE	IDENTIFIER
Deposited data		
Raw and analyzed data	This paper	GSE234704
Published code	This paper	https://github.com/valerievandenbempt/HAMSAB_singlecell
Experimental models: Cell lines		
Human: Embryonic Stem Cells (hESC) H1	WiCell	Cat# WAe001-A
Rat: INS-1E beta cell line	Dr Claes Wollheim	https://doi.org/10.1210/en.2003-1099
Experimental models: Organisms/strains		
Mouse: C57BL/6N	Charles River	Cat# 027C57BL/6
Mouse: Non-obese Diabetic (NOD) mice	Mathieu et al.	N/A
Mouse: NOD/Severe-Combined-Immunodeficiency	Jackson Laboratory	Cat# 001303
Oligonucleotides		
Primers listed in Table S2	This paper	N/A
Software and algorithms		
Seurat (v4.1.0)	R v4.2.2	https://satijalab.org/seurat/ RRID:SCR_016341
SingleCellExperiment (v1.12.0)	R v4.2.2	https://bioconductor.org/packages/SingleCellExperiment/ RRID:SCR_022493
scDBIFinder (v1.4.0)	R v4.2.2	https://bioconductor.org/packages/scDblFinder/
IntrinsicDimension package (v1.2.0)	R v4.2.2	https://CRAN.R-project.org/package=intrinsicDimension
Cluster package (v2.1.1)	R v4.2.2	https://CRAN.R-project.org/package=cluster
Rank Rank hypergeometric Overlap analysis	R v4.2.2	http://www.bioconductor.org/packages/release/bioc/html/RRHO.html RRID:SCR_022754
Gene set enrichment analysis (GSEA)	Broad institute	https://www.gsea-msigdb.org/gsea/index.jsp RRID:SCR_003199
Cell ranger pipeline	10X Genomics	https://support.10xgenomics.com/single-cell-gene-expression/software/pipelines/latest/what-is-cell-ranger RRID:SCR_017344
Prism version 9	Graphpad	http://www.graphpad.com RRID:SCR_002798
Fiji software (v2.3.0/1.53q)	ImageJ	https://imagej.nih.gov/ij/, 1997-2018 RRID:SCR_002285
FACSDiva software	BD biosciences	https://www.bdbiosciences.com/en-au/products/software/instrument-software/bd-facsdiva-software RRID:SCR_001456
FlowJo_v10.8.0	BD biosciences	https://www.flowjo.com/solutions/flowjo RRID:SCR_008520
NIS-Elements Confocal Software	Nikon Europe B.V.	https://www.microscope.healthcare.nikon.com/products/software/nis-elements/nis-elements-confocal RRID:SCR_014329
Other		
HAMS diet	This paper	Table S1
HAMSAB diet	This paper	Table S1
Chromium Controller	10X Genomics	N/A
NanoZoomer Digital Pathology	Hamamatsu Photonics	N/A

(*Continued on next page*)

Continued

REAGENT or RESOURCE	SOURCE	IDENTIFIER
Scanning Resonant AX-R Confocal microscope	Nikon Europe B.V.	N/A
FACSCanto™ flow cytometer	BD biosciences	N/A
Bio-Rad CFX96 machine	Bio-Rad laboratories	N/A
Amersham ImageQuant 800	Cytiva Life Science	N/A

RESOURCE AVAILABILITY

Lead contact

Further information and requests for resources and reagents should be directed and will be fulfilled by the lead contact, Esteban Gurzov (esteban.gurzov@ulb.be).

Materials availability

This study did not generate new unique reagents.

Data and code availability

- Single-cell RNA sequencing data have been deposited at GEO (GSE234704) and are publicly available as of the date of publication.
- This study did not generate original code.
- Microscopy data reported in this paper and any additional information required to reanalyse the data will be shared by the lead contact upon request.

EXPERIMENTAL MODEL AND STUDY PARTICIPANT DETAILS

Mice

NOD mice were housed and inbred in the animal facility of KU Leuven (Leuven, Belgium).[48] Diabetes incidence is higher in NOD females than in male mice,[48] thus 5-week-old female NOD mice were used for the study. C57BL/6N and NOD/Severe-Combined-Immunodeficiency (SCID) mice were housed and inbred in the animal facility of ULB (Brussels, Belgium). 8-10-week-old male and female C57BL/6N mice were used for pancreatic islet isolation. 8-10-week-old female NOD/SCID mice were used for human islet-like cell transplantation. All mice were housed under semi-barrier conditions, and animals were fed sterile food and water *ad libitum*. NOD mice were screened for the onset of diabetes by evaluating glucose levels in urine (Diastix Reagent Strips; Bayer, Leverkusen, Germany) and venous blood (AccuCheck; Roche Diagnostics, Vilvoorde, Belgium). Animals were maintained by the National Institutes of Health *Guide for the Care and Use of Laboratory Animals*, and all experimental procedures were approved and performed following the Animal Ethics Committee of the KU Leuven (P131/2019) and the Commission d'Ethique du Bien-être Animal of the ULB (reference 732N). Body weights and food intake were regularly monitored.

Cell cultures and treatments

Mouse islets were isolated according to previously published protocol[30] and treated *in vitro* with acetate (1mM) and/ or butyrate (1mM) for 1h prior to a treatment of mIFN-γ (1000U/mL, PeproTech, London, UK) and hIL-1β (50U/mL, R&D Systems, Minneapolis, MN) for 24h. Cell death was measured using SYTOX green (ThermoFisher Scientific, Scientific, Gibco, UK).

The insulin-producing INS-1E β-cell line was cultured as described.[49] Cytokine concentration (rIFN-γ 1000U/mL R&D Systems and hIL-1β 50U/mL) were selected based on previous time course and dose-response studies.[29,49] Sodium acetate or sodium butyrate (Sigma-Aldrich) were added to dose response and according to previous established concentrations.[6,8,33]

Human Embryonic Stem Cells (hESC) H1 (WiCell, Madison, WI) were cultured on plates coated with Matrigel (Corning BV, Amsterdam, the Netherlands) in Essential 8™ Medium (Life Technologies). hESC were differentiated into insulin-producing β-like cells (aggregates) in a 30-day protocol previously described.[29,30] NOD/SCID mice were anesthetized, and hESC-differentiated aggregates were implanted under the kidney capsule using a Hamilton syringe (Hamilton Bonaduz AG, Bonaduz, Switzerland). 200mM acetate and 150mM butyrate was added in their drinking water for one week. Circulating human C-peptide was measured in mouse plasma by ELISA (Mercodia, Uppsala, Sweden).

Cultured cells were regularly checked for mycoplasma contamination with MycoAlert® PLUS Mycoplasma Detection Kit (#LT07-705, Lonza, Basel, Switzerland).

METHOD DETAILS

In vivo procedures

Starting at 5 weeks of age, mice were randomly divided and fed *ad libitum* with two different diets (n=25-26 per dietary group): control HAMS (15% high amylose maize starch) and HAMSAB (15% acetylated and 15% butyrylated HAMS). NIH-31M (18% from protein, 45% from carbohydrate, and 6% from fat; Envigo, Indianapolis, IN) formula was used as base for preparing the supplemented diets (Table S1). Corn was

omitted, whereas wheat and oats were reduced to accommodate SCFA inclusion. Mice were fed with the diets for 5 weeks, then returned to the regular diet and diabetes incidence was monitored by 30 weeks of age or when reaching human endpoints. Mice were diagnosed as diabetic when they had glucosuria and two consecutive blood glucose measurements >200mg/dL. Evaluation of body and liver lean and fat mass was performed with EchoMRI™ 3-in-1 (NMR) body composition analyser from EchoMedical Systems (Houston, TX, USA).

Single-cell RNA sequencing sample preparation

5-week-old NOD mice were fed with HAMS (n=4) or HAMSAB (n=4) diet for 5 consecutive weeks. At the age of 10 weeks, pancreatic islets were isolated using collagenase (0.8 mg/mL, Sigma-Aldrich, St. Louis, MO) in Medium 199 (ThermoFisher Scientific, Gibco, UK). Histopaque-1077 (Sigma-Aldrich) was used to isolate the islets of Langerhans from debris and other tissue structures. The islets were dispersed into single cells using trypsin (10μL/mL, Sigma-Aldrich) and DNAseI (20μg/mL, Hofman-La Roche, Basel, Switzerland) in the dissociation media. Islet cells were filtered (40μM, Corning, BV, Amsterdam, The Netherlands) to remove clusters of cells. Live pancreatic islet cells were sorted by FACS using propidium iodide (1mg/mL, Sigma-Aldrich). After isolating and dispersing the islets, cells were pooled per condition to reach a significant cell number for further single-cell RNA sequencing analysis.

Bioinformatic analysis

The cells were loaded onto the chromium (10X Genomics, Pleasanton, CA) by the BRIGHT core facility (Brussels, Belgium), and libraries were prepared following the Chromium Single Cell 3' Reagent Kits User Guide. The resulting sequencing reads were aligned to the mm10 reference dataset (GRCm38) and demultiplexed using CellRanger. For data analysis, raw counts were filtered based on the number of genes (nFeature_RNA), as well as the percentage of mitochondrial genes (percent.mt). Cells with less than 100 nFeature_RNA, over 10% percent.mt, and genes expressed in less than 2 cells were excluded from the analysis. The remaining cells were converted into a "sce" object using the SingleCellExperiment package (v1.12.0) to facilitate doublet removal.[50] To remove doublets from the dataset, an unsupervised approach was used with the scDBlFinder package (v1.4.0). Finally, the cleaned data was analysed using Seurat (v4.1.0) in R (v4.0.4).[50]

The remaining 4117 and 4750 cells of HAMS and HAMSAB, respectively, were normalized using the SCTransform function with the top 1,000 variable features. This function returns the Pearson residuals from regularized negative binomial regression.[51] After normalization, the dimensions were reduced by Principal Component Analysis (PCA) and Uniform Manifold Approximation and Projection (UMAP). In UMAP, each dot represents a cell positioned based on its PCA values. The above steps were carried out separately for the HAMS-control diet and HAMSAB diet, and then merged into a single dataset using the merge function from Seurat. Clusters were annotated in a supervised manner based on cell signature markers in the literature. Further bioinformatic analysis was then performed on the merged dataset.

To perform in-depth analysis of separate cell types, the corresponding cluster was selected in a subset to compare gene expression and elucidate subclusters. For subclustering analysis, an unsupervised re-clustering approach was followed. The corresponding cell type cluster was subset from the entire dataset using the subset function from Seurat. To determine on the number of PCs required for PCA computation, the maxLikGlobalDimEst function was run using the IntrinsicDimension package (v1.2.0). The cluster package (v2.1.1) was then used to compute silhouette information according to a given clustering in k clusters and to decide the significant resolution to apply in UMAP.

Differential gene expression was performed for the subclusters using the FindAllMarkers function with default parameters in the standard Seurat pipeline. The top 10 genes obtained using the Wilcoxon rank-sum test are presented in dot, violin, or feature plots per cluster. Volcano plots, bar charts, and pie charts were generated using Prism software (GraphPad Software 9, La Jolla, CA). To map the proliferation profile of cells, the CellCycleScoring function was run using a list of cell cycle markers for G2M and S phases, which are preloaded in the Seurat package.

Single-cell RNA sequencing was performed on FACS-sorted immune cells in isolated islets from NOD mice, 4–12 mice per sample, at ages of 4 (infiltration), 8 (amplification) and 15 weeks (destruction).[14] This dataset can be found in the Gene Expression Omnibus database with accession number GSE141786. We normalised the datasets, and 2000 anchor features were used by CCA for integration to generate unsupervised UMAP plots.[52] The endothelial cells were removed from the comparison. The combined UMAP plot was used to compare Macrophages, T cells, cDC, β cells, α cells, δ cells and pDC.

To assess the interactions between ligand and receptor molecules, CellPhoneDB was used for cell communication analysis.[19] The input data was extracted and generated according to the documentation of CellPhoneDB. The mouse gene names were converted to human gene names prior to analysis using biomaRt. Significant mean and cell communication statistics (p-value < 0.05) were calculated based on the interaction and the normalised cell matrix achieved by Seurat normalisation. The dot plot was generated for all integrations between immune and endocrine cells for HAMS and HAMSAB displaying statistically significant results.

Rank-Rank Hypergeometric Overlap (RRHO) analysis of β cells was used to compare the HAMS diet to differential expressed genes in type 1 diabetic patients[26] as described previously.[29]

Histology and immunofluorescence

Mouse pancreata were fixed with formalin and embedded in paraffin, cut into 5 μm sections, and stained with haematoxylin and eosin. The stained slides were scanned with NanoZoomer Digital Pathology (Hamamatsu Photonics, Shizuoka, Japan; version SQ 1.0.9) at an original magnification of 40× and observed as well as graded by 3 double-blind reviewers. The 4 degrees of insulitis were judged according to the following criteria: Score 1, no visible islet infiltration, good islet morphology (round-shaped); Score 2, minor islet infiltration (<25%), preserved morphology; Score 3, major islet infiltration (>25%), preserved or slightly altered morphology; Score 4, islet completely infiltrated, altered islet morphology.

Parafilm sections were prepared for confocal microscopy as described previously.[30] Immunoblotting was performed using antibodies specified in the key resources table. The islets were imaged on Scanning Resonant AX-R Confocal microscope (Nikon Europe B.V., Amstelveen, The Netherlands) and processed using ImageJ® software (Version: 2.3.0/1.53q). The intensities were measured with the NIS-Element Confocal software (Nikon Europe B.V.). The fraction of cells expressing insulin was measured by immunofluorescence staining as previously described.[29,30]

Flow cytometry analysis

Single-cell suspensions of pancreatic lymph nodes (PLN) and the pancreas of HAMS- and HAMSAB-fed animals at 30 weeks of age were prepared as described.[53] Briefly, contaminating erythrocytes were removed from the dissociated single cells from PLN and the pancreas by incubating with red blood cell lysis buffer. Cells were subsequently stained with fluorophore-conjugated antibodies against the following molecules for Treg cells: CD3 (145-2C11), CD4 (GK1.5), CD8a (53-6.7), CD25 (PC61.5), and Foxp3 (FJK-16s). Cells were also stained with fluorophore-conjugated antibodies against the following molecules for activated T cells: CD3 (145-2C11), CD4 (GK1.5), CD8a (53-6.7), CD44 (IM7), and CD62L (MEL-14) (eBiosciences, Santa Clara, CA). Cells were then washed and acquired on a FACSCanto™ flow cytometer with FACSDiva software (BD Biosciences, Franklin Lakes, NJ). Data was exported as fcs files and analysed using FlowJo_v10.8.0 (BD Biosciences). Dead cells and doublets were excluded from the analysis.

Real-time PCR and Western blotting

Quantitative real-time PCR was performed using Bio-Rad CFX96 machine (Bio-Rad Laboratories, Hercules, CA) and SYBR Green reagent (Bio-Rad Laboratories). β-actin and/or GAPDH were used as internal controls. Probe and primer details are provided in key resources table and Table S2.

Immunoblotting was performed using antibodies specified the key resources table. Protein samples were collected in cell lysis buffer for western blot (Cell Signaling, Danvers, MA) and equivalent quantities of proteins were resolved by 12% SDS-PAGE and immunoblotted as indicated.[29] All blots were quantified using ImageJ2. Intensity values of the protein bands were normalized by the values of housekeeping protein GAPDH.

QUANTIFICATION AND STATISTICAL ANALYSIS

The results are presented as the mean ± standard error of the mean (SEM). Student's *t*-test was used for comparisons between the two groups. Differences among groups were assessed by two-way ANOVA or repeated-measures ANOVA. Statistical analyses were performed using Prism software (GraphPad Software). Sample size was predetermined based on the variability observed in prior experiments and on preliminary data. All experiments requiring the use of animals or animals to derive cells were subject to randomization based on litter.